An Experimental Study of a Solar Tomatoe Dryer Using Sierpinski Corrugated Carpets

Lohdy Diana
Department of Mechanics and Energy, Politeknik Elektronika Negeri Surabaya, Surabaya, Indonesia
lohdydiana@pens.ac.id (corresponding author)

Arrad Ghani Safitra
Department of Mechanics and Energy, Politeknik Elektronika Negeri Surabaya, Surabaya, Indonesia
arradgs@pens.ac.id

Eny Kusumawati
Department of Mechanics and Energy, Politeknik Elektronika Negeri Surabaya, Surabaya, Indonesia
eny-k@pens.ac.id

Firman Yunan Saputra
Department of Mechanics and Energy, Politeknik Elektronika Negeri Surabaya, Surabaya, Indonesia
firmanyunan123@pg.student.pens.ac.id

Aji Sukma Famuja Al Mali'in
Department of Mechanics and Energy, Politeknik Elektronika Negeri Surabaya, Surabaya, Indonesia
aji.maliin86@gmail.com

Received: 15 December 2025 | Revised: 14 January 2026 | Accepted: 28 January 2026

 DOI: https://doi.org/10.48084/etasr.16969

ABSTRACT

Solar dryers commonly have low heat transfer rates and non-uniform temperature distribution, which leads to reduced system efficiency. The performance of a solar dryer depends heavily on the design of the absorber plate, especially its ability to effectively capture and transfer solar heat. This study aims to enhance the efficiency of solar drying systems using tomatoes as the drying medium to provide a practical post-harvest processing solution for Indonesian farmers, who may experience significant financial losses during periods of drastic tomato price decline. The study used a Sierpinski carpet, a complex geometric structure, examining three fractal ratios (R_F), with values of 1.0, 0.75, and 0.6. Experiments were conducted in a controlled laboratory setting using a solar simulator. Their results indicate that the Sierpinski V-wave solar collector with an R_F of 0.6 achieved the highest thermal efficiency, obtaining a maximum value of 37.6%. Additionally, variations in radiation intensity were found to significantly influence the absorber plate temperature for the V-wave configuration. Compared with the other configuration, the maximum absorber plate temperature increased by approximately 9–12% among all evaluated designs. Overall, the results demonstrate that applying fractal-based Sierpinski carpet absorber plate designs, particularly with an R_F of 0.6, can significantly improve heat absorption and temperature distribution, increasing the efficiency of solar air heaters.

Keywords-solar energy; sierpinski carpet; absorber plate; thermal performance; efficiency

I. INTRODUCTION

Indonesia, in an effort to promote the development of the food processing sector, aims to enhance sustainable agricultural and plantation systems, one of which is fruit drying [1]. Traditional drying techniques, which rely on direct sunlight, have several limitations, including exposure to pests, insects, ultraviolet radiation, dust, and airborne particle contamination, resulting in practices that frequently fail to meet acceptable hygienic standards. Therefore, using solar radiation with solar air heaters is a more efficient and environmentally friendly alternative. Authors in [2] showed that variations in corrugated absorber designs can significantly improve thermal performance, with efficiency improvements reported as high as 67.83%. Reducing the temperature difference between the collector air and the surrounding environment decreases heat

loss, producing higher inlet air temperatures and increased collector efficiency. Authors in [3] investigated solar-powered tomato drying systems, using hot air supplied by solar air heaters for greenhouse drying, a method known as mixed-mode drying. Solar tunnel dryers equipped with tiered racks, fans, and Photovoltaic (PV) systems have been used to dry tomato slices [4]. Additionally, greenhouse-based drying systems have been evaluated from an economic perspective, including investment feasibility and analyses [5]. Authors in [6] used solar-powered tunnel dryers to examine drying performance and changes in the visual quality of tomatoes after drying. Authors in [7] reported that vitamin C degradation in tomato slices is influenced by drying temperature and slice thickness. Furthermore, hybrid solar tomato dryers have been reported to reduce energy consumption while improving product quality [8]. Thermal analyses of integrated PV and solar collector systems combined with greenhouse dryers have shown increases in overall efficiency of up to 17.69% [9]. In the present study, the absorber plate geometry was modified to a circular configuration. Conventional flat absorber plates generally have limited solar heat absorption capacity [10]. To improve this, the surface area of the plate was increased with a corrugated design, which increased the efficiency of solar drying systems [11]. This study used the Sierpinski concept, based on repeating fractal patterns with varying fractal ratios (FR). Authors in [12] used numerical simulations to analyze the behavior of external fluid flow through fractal structures. In addition to heat generation, solar dryers' performance is influenced by their capacity to store thermal energy over extended periods by integrating Phase Change Materials (PCMs) into solar collectors. PCMs store latent heat and maintain a nearly constant temperature during phase transitions [13, 14]. Authors in [15] reported maximum efficiencies of 33.67% with paraffin as the storage medium, during experiments on PCMs in tubes within solar collectors, which were also used to solar distillation systems [13, 16]. Indonesia's tropical climate, characterized by high humidity levels, poses additional challenges for drying applications because excessive moisture can negatively impact product quality. To mitigate this issue, moisture-absorbing materials are required; silica-based materials are among the most widely used [17, 18]. Authors in [19, 20] evaluated various desiccant materials, which exhibited significant moisture reduction when silica gel was used. This study contributes to existing literature by providing experimental evidence of the thermal benefits of using Sierpinski fractal geometry in the design of corrugated solar air heater absorber plates. The findings reveal a systematic correlation between variations in FR and improvements in absorber plate temperature, air thermal characteristics, and overall drying efficiency, extending current knowledge in this area.

II. THEORETICAL OF SOLAR DRYER PERFORMANCE

Solar dryers operate based on three processes: absorption of solar energy, heat transfer within the collector, and evaporation of moisture from agricultural products. The dryer prototype used for the experiment is shown in Figure 1 and consists of six main components: (1) an air inlet duct, (2) a glass cover, (3) a wooden collector housing, (4) a halogen lamp that serves as a solar radiation simulator, (5) a control panel, and (6) a drying chamber. Several interrelated parameters influence the drying system's overall performance, including the absorber plate's thermal behavior, the efficiency with which heat is transferred from the collector to the drying chamber, and the airflow's aerodynamic characteristics. The absorber plate captures solar radiation that passes through the transparent collector cover and converts it into sensible heat. Convective heat transfer then occurs between the heated absorber plate and the flowing air. This process is influenced by heat conduction within the absorber plate material and convective heat exchange at the plate–air interface. Modifications to the absorber plate's geometry are commonly used to improve its thermal performance. For example, corrugated surfaces with fractal perforations increase the effective heat absorption area and promote improved convective heat transfer. Consequently, the outlet air temperature rises, directly influencing the drying rate of the agricultural product. Heated air exits the collector and enters the drying chamber, where moisture is removed from the product surface due to the concentration gradient of moisture between the material and the drying air. This mechanism follows the coupled principles of heat and mass transfer. Evaporation is controlled by air temperature, airflow velocity, vapor pressure deficit, and the internal moisture diffusivity of the product. During the constant-rate drying period, moisture removal is primarily regulated by surface evaporation. During the falling-rate period, however, moisture transport can be described using Fick's diffusion law.

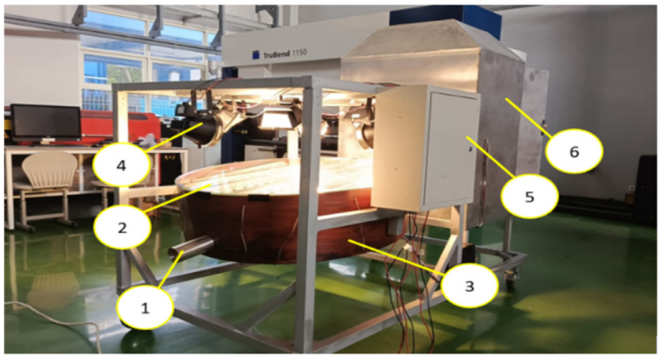

Fig. 1. Components of the solar dryer for tomato drying using Sierpinski corrugated carpet.

The overall thermal efficiency (ε) and the moisture content are:

$$\varepsilon = \frac{T_{out} - T_{in}}{T_{abs} - T_{in}} \quad (1)$$

$$Moisture\ Content = \frac{M_{wet} - M_{dry}}{M_{wet}} \times 100\ \% \quad (2)$$

where T_{out} is the air outlet temperature, T_{in} is the air inlet temperature, T_{abs} is the absorber surface temperature, M_{wet} is the wet mass, and M_{dry} is the dry mass. The efficiency of a solar collector is strongly influenced by the absorber plate's thermal capability, solar radiation intensity, insulation quality, and airflow distribution. Using fractal structures, such as Sierpinski carpets, into corrugated absorber plates generates complex airflow pathways, enhancing natural convection and promoting

a more uniform temperature distribution. Improving heat distribution is essential for achieving consistent and efficient drying performance. Additionally, integrating thermal energy storage materials, such as PCMs or silica-based desiccants, extends heat availability during periods of low solar radiation and assists with humidity control within the drying chamber. These materials store excess thermal energy during peak solar conditions and gradually release it over time, thereby stabilizing drying temperatures and improving energy and exergy efficiency overall.

III. MATERIALS AND EXPERIMENTAL TEST PROCEDURE

The experimental setup consists of a solar collector, a drying cabinet, and a solar simulator circuit. The Sierpinski Corrugated Carpet Solar Air Heater (SCCA-SAH) works by allowing solar radiation to pass through the glass cover and be absorbed by the Sierpinski carpet absorber plate, illustrated in Figure 2. Some of the absorbed heat is transmitted through the fractal gaps in the plate, which warms the air entering through the four inlet openings at the bottom of the collector.

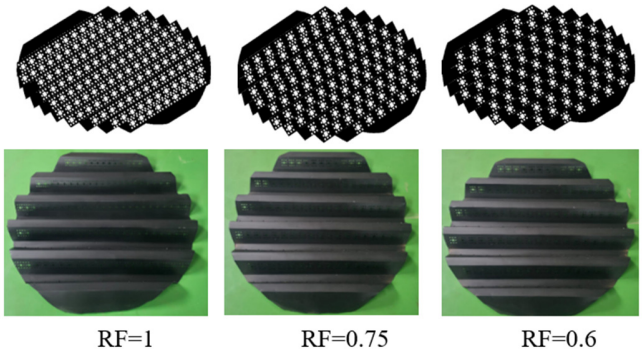

Fig. 2. Variations of Sierpinski corrugated carpets.

The incoming air naturally moves upwards through the fractal gaps due to buoyancy effects. The air is heated in two stages: first, it comes into contact with the lower surface of the Sierpinski carpet absorber plate, where heat is transferred through conduction and natural convection. Subsequently, the air is reheated as it passes through the fractal gaps and interacts with the upper surface of the absorber plate. The heated air leaving the collector is directed into a drying cabinet for drying tomatoes. Within the cabinet, the hot air circulates upward through the gaps between the shelves, ensuring uniform contact with the tomato samples. The exhaust air subsequently exits through the top of the cabinet, as demonstrated in the diagram of Figure 2. The specifications of the measuring instruments used in the experiment are portrayed in Table I. In this study, geometric variation is defined by the length-to-distance ratio, referred to as the fractal ratio R_F. Three R_F configurations were investigated: $R_{F1} = 1.0$, $R_{F2} = 0.75$, and $R_{F3} = 0.6$.

IV. RESULTS AND DISCUSSION

A. *Effect of Absorber Temperature on Time and Radiation Intensity*

Figure 4 shows how absorber plate temperature changes over time and in relation to solar radiation intensity during the testing of the three collector configurations. The graph displays the relationship between solar radiation intensity and absorber plate temperature. An increase in temperature for each configuration indicates the absorber design's effectiveness in capturing solar heat.

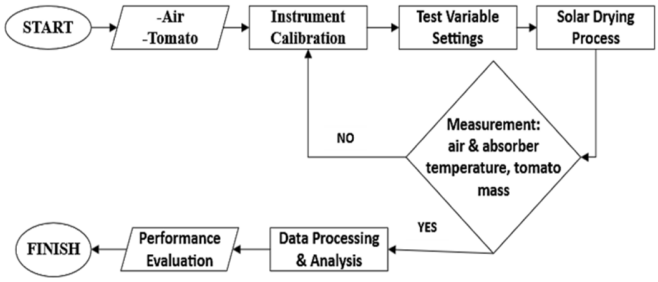

Fig. 3. Schematic diagram of the experimental method.

TABLE I. SPESIFICATIONS

Measuring instruments	Specifications
Thermometer (PT-100)	Temperature range: -50°C to 250°C; precision: ±0.1°C
Anemometer	Measurement range: 0.4–20 m/s;
Pyranometer	Measurement range: 0–2000 W/m²; sensitivity: 7–14 µV/W/m²
Digital moisture meter	Moisture range: 5–30%; humidity: 5%–90%

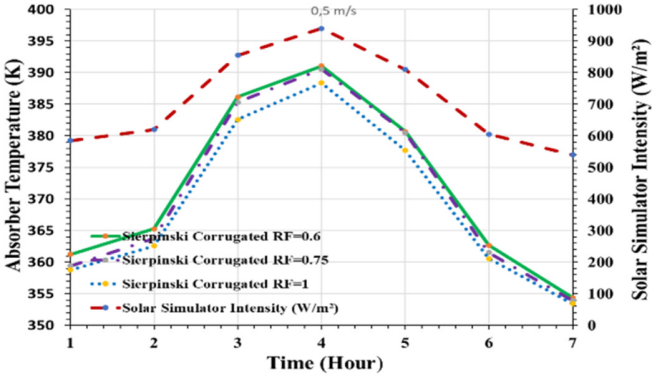

Fig. 4. Effect of radiation intensity and time on absorber plate temperature.

Variations in radiation intensity occur because incident solar radiation is not constant, but is highly influenced by operating conditions, resulting in fluctuations in the collector outlet temperature. Figure 4 presents the trend of absorber plate temperature variations, demonstrating that the primary driving force for temperature increases within the absorber plate is the radiation intensity generated by the solar simulator. As radiation intensity gradually increased from 585 W/m² to 945 W/m², all three Sierpinski wave absorber configurations exhibited a significant, almost linear increase in temperature,

rising from approximately 350 K to 400 K. This behavior confirms the absorber plate temperature's strong dependence on incident radiation intensity under controlled experimental conditions. Throughout testing, the R_F = 0.6 configuration exhibited the highest absorber plate temperature at all radiation intensity levels, followed by the R_F = 0.75 and R_F = 1.0 configurations, indicating that is more capable of capturing and retaining incident radiation energy. The results show that the absorber plate temperature is significantly influenced by the heat transfer surface area, which is controlled by the FR. Absorber plates with fewer, widely spaced perforations absorb heat more effectively than plates with many closely spaced perforations. Corrugated absorber plates enhance heat transfer by increasing the effective surface area and inducing airflow turbulence. Furthermore, using a Sierpinski fractal pattern increases the effective heat transfer area without significantly increasing mass or airflow resistance, thereby improving heat absorption efficiency. As air flows through proportionally spaced perforations, heat distribution occurs more rapidly, resulting in higher outlet air temperatures. The superior thermal performance of the R_F = 0.6 configuration indicates that an optimized fractal structure with perforation spacing promotes more effective interaction between radiation absorption, convective heat transfer, and absorber surface geometry. This optimized configuration enables efficient heat absorption while maintaining stable airflow pathways.

B. Changes in Thermal Conductivity of Air in the Collector with Time

Figure 5 shows how collector design affects the thermal conductivity of air within the collector. The latter noticeably increases over time for all tested configurations. Initially, the thermal conductivity ranges from approximately 30 - 31 × 10^{-3} W/m·K, subsequently increasing to values exceeding 33 × 10^{-3} W/m·K. This indicates that the air becomes more effective at conducting heat as the system operates, which is closely associated with the rise in operating temperature inside the collector.

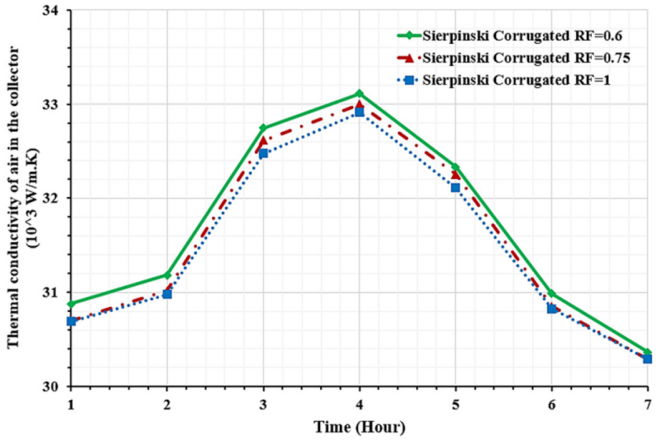

Fig. 5. Variation of air thermal conductivity in the collector with time.

The collector with R_F = 1.0, which has the highest number of perforations, exhibits relatively lower performance compared to the other configurations. This design achieves a maximum air thermal conductivity of approximately 32 × 10^{-3} W/m·K. In contrast, the R_F = 0.6 configuration demonstrates the highest thermal conductivity, approaching 33 × 10^{-3} W/m·K, followed by the R_F = 0.75 configuration. These results suggest that temporal changes in air thermal conductivity are strongly influenced by temperature variations resulting from differences in collector geometry. Additionally, the interaction between fractal geometry and airflow significantly impacts air thermal conductivity, directly affecting collector performance. More complex absorber plate geometries, such as the Sierpinski pattern, increase the effective heat transfer area and enhance airflow turbulence, enhancing the effective thermal conductivity of air, leading to increased heating efficiency.

C. Changes in Heat Transfer Coefficient with Time

Figure 6 shows that the Sierpinski collector plate with RF = 1.0 has the highest convective heat transfer coefficient. An increase in fluid density allows more air to carry thermal energy, which increases the convective heat transfer coefficient (h) and the overall convective heat transfer rate. Higher values of h, the rate of heat transfer between the absorber plate surface and the flowing air, indicate more effective convection and faster moisture removal from the dried material. Typically, free convective heat transfer coefficients range from 2 W/m²·K to 25 W/m²·K, and the values obtained in this study fall within this range [9]. Variations in fractal geometry density influence the thermal contact between heated air and the absorber surface, improving heat release and supporting a more rapid drying process.

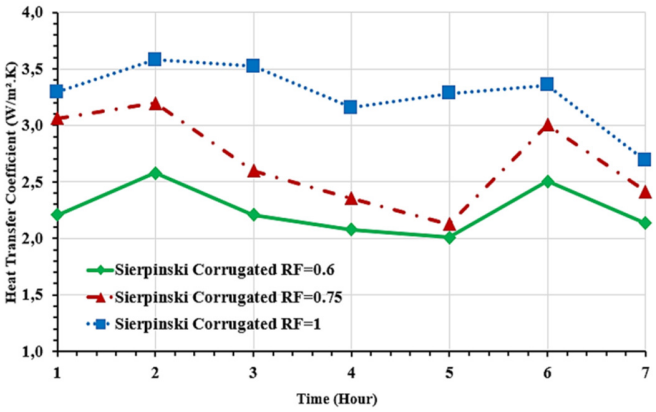

Fig. 6. Variation of the heat transfer coefficient in the collector with time.

D. Changes in Moisture Content with Time

The moisture content of tomatoes during the drying process is affected by the ambient temperature and humidity as well as the material properties [10]. Figure 7 shows the moisture content of the tomatoes calculated using (2), with lower final tomato weight indicating higher moisture content values. The moisture content varies with drying time over 7 h for different Sierpinski carpet corrugated configurations. An almost linear increase in moisture removal is observed with drying time for all configurations. However, the drying rate is determined by the FR. After 7 h, the R_F = 0.6 configuration had the highest moisture removal at 23%, followed by R_F = 0.75 at 20% and R_F

= 1 at 19%. Under identical drying conditions, moisture removal increases by 15–20% for R_F = 0.6 compared to R_F = 1, and by 10–12% compared to R_F = 0.75. The superior performance of the R_F = 0.6 configuration is evident from the early drying stage. After 3 h, moisture removal reaches 11%, while values of 10% and 9% are obtained for the R_F = 0.75 and R_F = 1 configurations, respectively. These results confirm that a higher initial drying rate is achieved with R_F = 0.6, resulting in reduced overall drying time. Drying occurs due to differences in water vapor concentration between the incoming drying air and the exhaust air leaving the outlet duct [11].

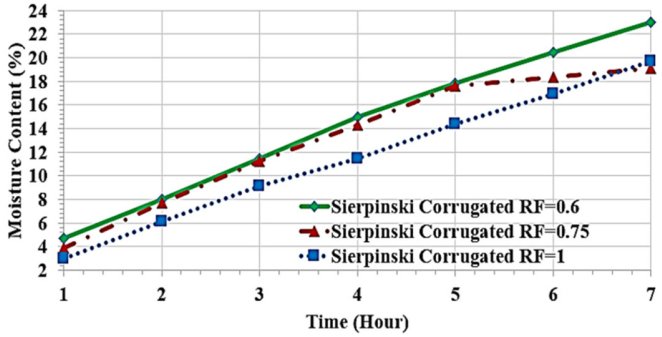

Fig. 7. Effect of absorber plate temperature on tomato moisture content.

E. Changes in Thermal Effectiveness with Time

The Sierpinski wave collector with R_F = 0.6 exhibited the highest collector efficiency over time during the 6th h of testing, reaching a value of 37.2%. In contrast, the lowest efficiency, 19.8%, was recorded for the R_F = 1.0 configuration. Figure 8 illustrates the thermal efficiency, which is defined as the ratio of the useful heat energy gained by the collector to the incident solar radiation (I, in W/m²).

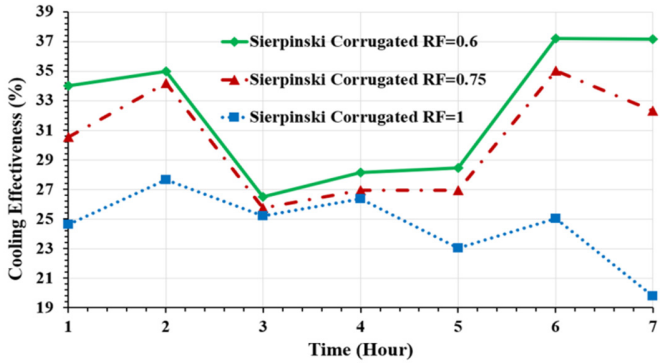

Fig. 8. Variation of collector effectiveness with time.

Solar air heater performance can be effectively evaluated using thermal efficiency, which is expressed as the ratio of the actual temperature increase of the working fluid to the maximum possible temperature increase under identical operating conditions [7]. In this context, thermal efficiency represents the system's capability to absorb solar energy and transfer it to the airflow while minimizing heat losses. The thermal effectiveness (ε) of a solar air heater is defined as the ratio of the heat energy absorbed by the working fluid to the solar energy incident on the collector surface [12]. Thermal efficiency and thermal effectiveness are both important indicators of collector performance. Improving the heat transfer rate between the absorber surface and the working fluid can enhance collector efficiency. This can be achieved by increasing the airflow rate, using working fluids with higher thermal conductivity, or optimizing the absorber surface design [13].

F. Changes in Collector Efficiency with Time

Figure 9 shows how efficiently solar air collectors convert incoming solar radiation into useful thermal energy. This efficiency represents the collector's ability to absorb solar heat and transfer it to the air flowing through the system. Thermal efficiency is typically expressed as a percentage and is calculated based on parameters such as the amount of heat gained by the air and the corresponding airflow rate [14]. Several factors influence the thermal performance of a solar air collector, including solar radiation intensity, ambient temperature, outlet air temperature, and airflow rate. Additionally, the orientation of the absorber plate substantially impacts the collector's overall thermal efficiency [15]. The present study reveals that the orientation of the absorber plate is crucial for enhancing heat transfer and improving the performance of the collector. This behavior is evident in the Sierpinski configuration with R_F = 0.6, which exhibits the highest efficiency during the 1st and 2nd h of operation. However, the highest efficiency is observed for the R_F = 1.0 configuration during the 3rd and 4th h. These variations can be attributed to differences in geometric orientation, such as hole diameter and spacing between holes perpendicular to the airflow direction. These factors were analyzed to determine their contribution to enhancing thermal efficiency. Additionally, the arrangement and pattern of the Sierpinski carpet were evaluated to optimize heat transfer characteristics and increase the outlet air temperature of the solar air collector.

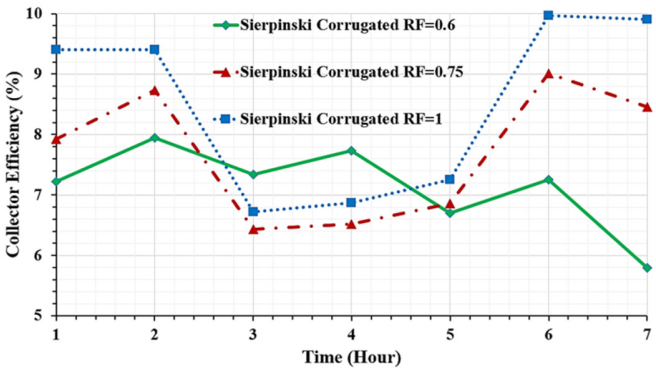

Fig. 9. Variation of collector efficiency with time.

G. Tomato Dry Test

Figure 10 depicts the drying results for all Sierpinski configurations. The R_F = 0.6 configuration has the most effective drying performance, with the final moisture content of the tomatoes being lower than with the other two configurations. These differences in drying outcomes indicate

that variations in inter-fractal spacing significantly influence heat distribution and the overall effectiveness of the drying process. The experimental results also suggest that fractal geometry affects airflow characteristics and enhances heat transfer to the material surface. With more optimal fractal spacing, corresponding to R_F = 0.6, heat is distributed more uniformly, allowing the evaporation process to occur more rapidly. These results underscore the importance of fractal-based absorber plate design in enhancing the efficiency of solar drying systems.

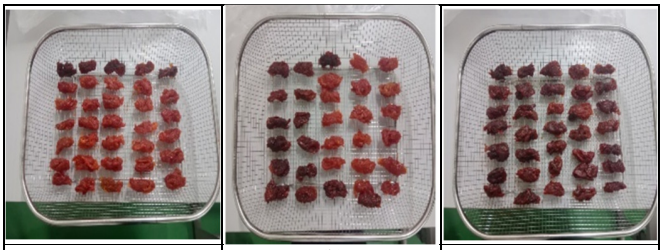

(a) (b) (c)

Fig. 10. Tomatoes after drying: (a) R_F = 1.0, (b) R_F = 0.75, and (c) R_F = 0.6.

V. CONCLUSIONS

The following conclusions can be drawn based on the analysis and discussion presented in this study:

- The R_F = 0.6 configuration exhibited the best thermal performance among all configurations tested, with the maximum absorber plate temperature increasing by 9%–12%.
- The V-wave Sierpinski solar collector with R_F = 0.6 achieved the highest thermal effectiveness, reaching a maximum value of 37.6%.
- Variations in solar radiation intensity were found to significantly influence the absorber plate temperature of solar collectors with V-wave absorber plates. Among the tested configurations, the Sierpinski carpet absorber with an R_F value of 0.6 recorded the highest temperature, reaching 117.4 °C.

While promising results were obtained, future work should include testing under direct sunlight and exploring alternative fractal absorber designs. Additionally, maintaining stable temperature conditions within the drying chamber is proposed, as well as investigating forced convection and integrating thermal energy storage systems to enhance overall performance.

ACKNOWLEDGMENT

This research was funded by the Directorate of Research and Community Service (Direktorat Penelitian dan Pengabdian Masyarakat, DPPM) and supported by the Electronics Engineering Polytechnic Institute of Surabaya (Politeknik Elektronika Negeri Surabaya, PENS).

REFERENCES

[1] M. T. Sambodo *et al.*, "Breaking barriers to low-carbon development in Indonesia: deployment of renewable energy, " *Heliyon*, vol. 8, no. 4, Apr. 2022, Art. no. e09304, https://doi.org/10.1016/j.heliyon.2022.e09304.

[2] W. Zheng, "Experimental investigation of the transpired solar air collectors and metal corrugated packing solar air collectors," *Energies*, vol. 10, no. 3, Mar. 2017, Art. no. 302, https://doi.org/10.3390/en10030302.

[3] A. Djebli and O. Badaoui, "A new approach to the thermodynamics study of drying tomatoes in mixed solar dryer," *Solar Energy*, vol. 193, pp. 164–174, Sep. 2019, https://doi.org/10.1016/j.solener.2019.09.057.

[4] L. T. Dufera, "Experimental evaluation of drying kinetics of tomato (*Lycopersicum esculentum* L.) slices in twin layer solar tunnel dryer," *Environmental and Sustainability Indicators*, vol. 61, pp. 241–250, Mar. 2021, https://doi.org/10.1016/j.esd.2021.03.003.

[5] B. Duraivel, N. Muthuswamy, and S. Gnanavendan, "Comprehensive analysis of the greenhouse solar tunnel dryer (GSTD) using tomato, snake gourd, and cucumber: Insights into energy efficiency, exergy performance, economic viability, and environmental impact," *Solar Energy*, vol. 267, Dec. 2023, Art. no. 112263, https://doi.org/10.1016/j.solener.2023.112263.

[6] C. Deepak, "Experimental analysis of a mixed mode solar tunnel dryer for drying tomato: Energy, exergy and environmental assessment," *Thermal Science and Engineering Progress*, vol. 63, May 2025, Art. no. 103707, https://doi.org/10.1016/j.tsep.2025.103707.

[7] H. Ebadi, "Performance of a hybrid compound parabolic concentrator solar dryer for tomato slices drying," *Solar Energy*, vol. 215, pp. 44–63, Jan. 2021, https://doi.org/10.1016/j.solener.2020.12.026.

[8] M. Sharma, "Performance evaluation of indirect type domestic hybrid solar dryer for tomato drying: Thermal, embodied, economical and quality analysis," *Thermal Science and Engineering Progress*, vol. 42, Apr. 2023, Art. no. 101882, https://doi.org/10.1016/j.tsep.2023.101882.

[9] M. M. Azam, "Thermal analysis of PV system and solar collector integrated with greenhouse dryer for drying tomatoes," *Energy*, vol. 212, Dec. 2020, Art. no. 118764, https://doi.org/10.1016/j.energy.2020.118764.

[10] N. B. Khedher, "Experimental Evaluation of a Flat Plate Solar Collector Under Hail City Climate," *Engineering, Technology & Applied Science Research*, vol. 8, no. 2, pp. 2750–2754, Apr. 2018, https://doi.org/10.48084/etasr.1957.

[11] B. A. Dwiyantoro and A. Fakhruddin, "A Numerical Study on the Improvement of the Thermal Performance of a Solar Chimney Power Plant with Variation in the Absorber," *Engineering, Technology & Applied Science Research*, vol. 15, no. 5, pp. 27452–27463, Oct. 2025, https://doi.org/10.48084/etasr.12483.

[12] M. Mohammad and A. Trounev, "Fractal-induced flow dynamics: Viscous flow around Mandelbrot and Julia sets," *Chaos, Solitons & Fractals*, vol. 199, Oct. 2025, Art. no. 1166195, https://doi.org/10.1016/j.chaos.2025.116619.

[13] R. Bahramei, "Thermo-economic evaluation of a solar desalination equipped with phase change material and spraying unit," *Desalination*, vol. 574, 2024, Art. no. 117197, https://doi.org/10.1016/j.desal.2023.117197.

[14] A. Das, M. M. H. Apu, A. Akter, M. M. Al Reza, and R. Mia, "An overview of phase change materials, their production, and applications in textiles," *Results in Engineering*, vol. 25, 2025, Art. no. 103603, https://doi.org/10.1016/j.rineng.2024.103603.

[15] Y. Gunawan, I. A. N. T. Trisnadewi, and N. Putra, "Performance of natural wax as phase change material for intermittent solar energy storage in agricultural drying: An experimental study," *Solar Energy*, vol. 251, pp. 158–170, Feb. 2023, https://doi.org/10.1016/j.solener.2023.01.008.

[16] J. Seifi, "Investigating the thermo-economic performance and modeling of a parabolic solar collector with phase change material in the receiver tube in a solar desalination," *Desalination*, vol. 572, 2024, Art. no. 116980, https://doi.org/10.1016/j.desal.2023.116980.

[17] P. Kavitharani, J. Janet, S. Venkata Lakshmi, S. Hemamalini, and S. Marichamy, "Experimental analysis for moisture sensing system on silica sand using IoT approach," *Materials Today: Proceedings*, vol. 45, pp. 2416–2418, 2021, https://doi.org/10.1016/j.matpr.2020.10.837.

[18] W. Dong, "Study on durability and water absorption characteristics of nano silica modified aeolian sand concrete in salt freezing environment," *Materials Today Communications*, vol. 47, 2025, Art. no. 113148, https://doi.org/10.1016/j.mtcomm.2025.113148.

[19] X. Xiao, Z. Han, Y. Wang, and M. Li, "Thermal characterization and moisture adsorption performance of calcium alginate hydrogel/silica gel/polyvinylpyrrolidone/expanded graphite composite desiccant," *Cleaner Engineering and Technology*, vol. 13, 2024, Art. no. 100323, https://doi.org/10.1016/j.ccst.2024.100323.

[20] L. D. V. Anand, S. S. P. Kamala, D. Hepsiba, D. Ravikumar, A. Jayapradha, and S. Marichamy, "Experimental analysis on effect of infrared light source for moisture content test of silica sand," *Materials Today: Proceedings*, vol. 45, pp. 2289–2292, 2021, https://doi.org/10.1016/j.matpr.2020.10.268